Research in Astron. Astrophys. **2010** Vol. **XX** No. **XX**, 000–000
http://www.raa-journal.org *http://www.iop.org/journals/raa*

***R**esearch in*
***A**stronomy and*
***A**strophysics*

Influence of scalar-isovector δ-meson field on quark phase structure in neutron stars

G.B. Alaverdyan

Yerevan State University, Yerevan 0025, Armenia; *galaverdyan@ysu.am*

Received [2010] [month] [day]; accepted [year] [month] [day]

Abstract The deconfinement phase transition from hadronic matter to quark matter in the interior of compact stars is investigated. The hadronic phase is described in the framework of relativistic mean-field (RMF) theory, when also the scalar-isovector δ-meson effective field is taken into account. The MIT bag model for describing a quark phase is used. The changes of the parameters of phase transition caused by the presence of δ-meson field are explored. Finally, alterations in the integral and structural parameters of hybrid stars due to both deconfinement phase transition and inclusion of δ-meson field are discussed.

Key words: Equation of state: mean-field: neutron stars: quarks: deconfinement phase transition

1 INTRODUCTION

The structure of compact stars functionally depends on the equation of state (EOS) of matter in a sufficiently wide range of densities - from 7.9 g/cm^3 (the endpoint of thermonuclear burning) to one order of magnitude higher than nuclear saturation density. Therefore, the study of properties and composition of the matter constituents at extremely high density region is of a great interest in both nuclear and neutron star physics. The relativistic mean-field (RMF) theory (Walecka 1974; Serot & Walecka 1986, 1997) has been effectively applied to describe the structure of finite nuclei (Lalazissis et al. 1997; Typel & Wolter 1997), the features of heavy-ion collisions (Ko & Li 1996; Prassa et al. 2007), and the equation of state (EOS) of nuclear matter (Miller & Serot 1995). Inclusion of the scalar-isovector δ-meson in this theoretical scheme and investigation of its influence on low density asymmetric nuclear matter was realized in Refs. Kubis & Kutschera (1999); Liu et al. (2002); Greco et al. (2003). At sufficiently high density, different exotic degrees of freedom, such as pion and kaon condensates, also deconfined quarks, may appear in the strongly interacting matter. The modern concept of hadron-quark phase transition is based on the feature of that transition, that is the presence of two conserved quantities in this transition: baryon number and electric charge (Glendenning 1992). It is known that, depending on the value of surface tension, σ_s, the phase transition of nuclear matter into quark matter can occur in two scenarios (Heiselberg et al. 1993; Heiselberg & Hjorth-Jensen 1999): ordinary first order phase transition with a density jump (Maxwell construction), or formation of a mixed hadron-quark matter with a continuous variation of pressure and density (Glendenning construction) (Glendenning 1992). Uncertainty of the surface tension values does not allow to determine the phase transition scenario, taking place in reality. In our recent paper (Alaverdyan 2009a) in the assumption that the transition to quark matter is a usual first-order phase transition, described by Maxwell construction, we have shown that the presence of the δ-meson field leads to the decrease of transition pressure P_0, of baryon number densities n_N and n_Q.

In this article we investigate the hadron-quark phase transition of neutron star matter, when the transition proceeds through a mixed phase. The calculations results of the mixed phase structure (Glendenning construction) are compared with the results of usual first-order phase transition (Maxwell construction). Also influence of δ-meson field on phase transition characteristics is discussed. Finally, using the EOS obtained, we calculate the integral and structural characteristics of neutron stars with quark degrees of freedom.

2 NEUTRON STAR MATTER EQUATION OF STATE

2.1 Nuclear Matter

In this section we consider the EOS of matter in the region of nuclear and supranuclear density ($n \geq 0.1$ fm^{-3}). For the lower density region, corresponding to the outer and inner crust of the star, we have used the EOS of Baym-Bethe-Pethick (BBP) (Baym et al. 1971). To describe the hadronic phase we use the relativistic nonlinear Lagrangian density of many-particle system consisted of nucleons, p, n, electrons and isoscalar-scalar (σ), isoscalar-vector (ω), isovector-scalar (δ), and isovector-vector (ρ) - exchanged mesons:[1]

$$\begin{aligned}\mathcal{L} = \overline{\psi}_N[\gamma^\mu(i\partial_\mu - g_\omega\omega_\mu(x) - \frac{1}{2}g_\rho \overrightarrow{\tau}_N \overrightarrow{\rho}_\mu(x)) - (m_N - g_\sigma\sigma(x) - g_\delta \overrightarrow{\tau}_N \overrightarrow{\delta}(x))]\psi_N \\ +\frac{1}{2}(\partial_\mu\sigma(x)\partial^\mu\sigma(x) - m_\sigma\sigma(x)^2) - U(\sigma(x)) + \frac{1}{2}m_\omega^2\omega^\mu(x)\omega_\mu(x) - \frac{1}{4}\Omega_{\mu\nu}(x)\Omega^{\mu\nu}(x) \\ +\frac{1}{2}(\partial_\mu \overrightarrow{\delta}(x)\partial^\mu \overrightarrow{\delta}(x) - m_\delta^2 \overrightarrow{\delta}(x)^2) + \frac{1}{2}m_\rho^2 \overrightarrow{\rho}^\mu(x)\overrightarrow{\rho}_\mu(x) - \frac{1}{4}\Re_{\mu\nu}(x)\Re^{\mu\nu}(x) \\ +\overline{\psi}_e(i\gamma^\mu\partial_\mu - m_e)\,\psi_e, \qquad (1)\end{aligned}$$

where $x = x_\mu = (t, x, y, z)$, $\sigma(x)$, $\omega_\mu(x)$, $\overrightarrow{\delta}(x)$, and $\overrightarrow{\rho}^\mu(x)$ are the fields of the σ, ω, δ, and ρ exchange mesons, respectively, $U(\sigma)$ is the nonlinear part of the potential of the σ-field, given by Boguta & Bodmer 1977

$$U(\sigma) = \frac{b}{3}\, m_N(g_\sigma\sigma)^3 + \frac{c}{4}\,(g_\sigma\sigma)^4, \qquad (2)$$

m_N, m_e, m_σ, m_ω, m_δ, m_ρ are the masses of the free particles, $\psi_N = \begin{pmatrix}\psi_p \\ \psi_n\end{pmatrix}$ is the isospin doublet for nucleonic bispinors, and $\overrightarrow{\tau}$ are the isospin 2×2 Pauli matrices. The symbol "$\rightarrow$" denote vectors in isotopic spin space. This Lagrangian also includes antisymmetric tensors of the vector fields $\omega_\mu(x)$ and $\overrightarrow{\rho}_\mu(x)$ given by

$$\Omega_{\mu\nu}(x) = \partial_\mu\omega_\nu(x) - \partial_\nu\omega_\mu(x), \qquad \Re_{\mu\nu}(x) = \partial_\mu\overrightarrow{\rho}_\nu(x) - \partial_\nu\overrightarrow{\rho}_\mu(x). \qquad (3)$$

In the RMF theory, the meson fields $\sigma(x)$, $\omega_\mu(x)$, $\overrightarrow{\delta}(x)$ and $\overrightarrow{\rho}_\mu(x)$ are replaced by the effective mean-fields $\overline{\sigma}$, $\overline{\omega}_\mu$, $\overrightarrow{\overline{\delta}}$ and $\overrightarrow{\overline{\rho}}_\mu$.

This Lagrangian density (1) contains the meson-nucleon coupling constants, g_σ, g_ω, g_ρ and g_δ, also parameters of σ-field self-interacting terms, b and c. In our calculations we take for the δ coupling constant, $a_\delta = (g_\delta/m_\delta)^2 = 2.5$ fm^2, as in Refs. Liu et al. (2002); Greco et al. (2003); Alaverdyan (2009a), for the bare nucleon mass, $m_N = 938.93$ MeV, for the nucleon effective mass, $m_N^* = 0.78\, m_N$, for the baryon number density at saturation, $n_0 = 0.153$ fm^{-3}, for the binding energy per baryon, $f_0 = -16.3$ MeV, for the incompressibility modulus, $K = 300$ MeV, and for the asymmetry energy, $E_{sym}^{(0)} = 32.5$ MeV. Five other constants $a_\sigma = (g_\sigma/m_\sigma)^2$, $a_\omega = (g_\omega/m_\omega)^2$, $a_\rho = (g_\rho/m_\rho)^2$, b and c then can be numerically determined (Alaverdyan 2009a).

[1] We use the natural system of units with $\hbar = c = 1$.

Table 1 Model Parameters with and without δ -Meson Field

	a_σ (fm^2)	a_ω (fm^2)	a_δ (fm^2)	a_ρ (fm^2)	b (fm^{-1})	c
$RMF\sigma\omega\rho\delta$	9.154	4.828	2.5	13.621	$1.654 \cdot 10^{-2}$	$1.319 \cdot 10^{-2}$
$RMF\sigma\omega\rho$	9.154	4.828	0	4.794	$1.654 \cdot 10^{-2}$	$1.319 \cdot 10^{-2}$

In Table 1 we list the values of the model parameters with and without the isovector-scalar δ meson interaction channel (The models $RMF\sigma\omega\rho\delta$ and $RMF\sigma\omega\rho$, respectively).

The knowledge of the model parameters makes it possible to solve the set of four equations in a self-consistent way and to determine the re-denoted mean-fields, $\sigma \equiv g_\sigma \bar{\sigma}$, $\omega \equiv g_\omega \bar{\omega_0}$, $\delta \equiv g_\delta \bar{\delta}^{(3)}$, and $\rho \equiv g_\rho \bar{\rho_0}^{(3)}$, depending on baryon number density n and asymmetry parameter $\alpha = (n_n - n_p)/n$. The standard QHD procedure allows to obtain expressions for energy density $\varepsilon(n,\alpha)$ and pressure $P(n,\alpha)$ of nuclear npe plasma:

$$\begin{aligned}\varepsilon_{NM}(n,\alpha,\mu_e) = \frac{1}{\pi^2}\int\limits_0^{k_-(n,\alpha)} \sqrt{k^2 + m_p^*(\sigma,\delta)^2}\, k^2 dk \\ + \frac{1}{\pi^2}\int\limits_0^{k_+(n,\alpha)} \sqrt{k^2 + m_n^*(\sigma,\delta)^2}\, k^2 dk \\ + \frac{b}{3} m_N \sigma^3 + \frac{c}{4}\sigma^4 + \frac{1}{2}\left(\frac{\sigma^2}{a_\sigma} + \frac{\omega^2}{a_\omega} + \frac{\delta^2}{a_\delta} + \frac{\rho^2}{a_\rho}\right) \\ + \frac{1}{\pi^2}\int\limits_0^{\sqrt{\mu_e^2 - m_e^2}} \sqrt{k^2 + {m_e}^2}\, k^2 dk, \end{aligned} \tag{4}$$

$$\begin{aligned}P_{NM}(n,\alpha,\mu_e) = \frac{1}{\pi^2}\int\limits_0^{k_-(n,\alpha)} \left(\sqrt{k_-(n,\alpha)^2 + m_p^*(\sigma,\delta)^2} - \sqrt{k^2 + m_p^*(\sigma,\delta)^2}\right) k^2 dk \\ + \frac{1}{\pi^2}\int\limits_0^{k_+(n,\alpha)} \left(\sqrt{k_+(n,\alpha)^2 + m_n^*(\sigma,\delta)^2} - \sqrt{k^2 + m_n^*(\sigma,\delta)^2}\right) k^2 dk \\ - \frac{b}{3} m_N \sigma^3 - \frac{c}{4}\sigma^4 + \frac{1}{2}\left(-\frac{\sigma^2}{a_\sigma} + \frac{\omega^2}{a_\omega} - \frac{\delta^2}{a_\delta} + \frac{\rho^2}{a_\rho}\right) \\ + \frac{1}{3\pi^2}\mu_e\left(\mu_e^2 - m_e^2\right)^{3/2} - \frac{1}{\pi^2}\int\limits_0^{\sqrt{\mu_e^2 - m_e^2}} \sqrt{k^2 + {m_e}^2}\, k^2 dk, \end{aligned} \tag{5}$$

where μ_e is the chemical potential of electrons,

$$m_p^*(\sigma,\delta) = m_N - \sigma - \delta, \quad m_n^*(\sigma,\delta) = m_N - \sigma + \delta \tag{6}$$

are the effective masses of the proton and neutron, respectively, and

$$k_\pm(n,\alpha) = \left(\frac{3\pi^2 n}{2}(1 \pm \alpha)\right)^{1/3}. \tag{7}$$

The chemical potentials of the proton and neutron are given by

$$\mu_p(n,\alpha) = \sqrt{k_-(n,\alpha)^2 + m_p^*(\sigma,\delta)^{\,2}} + \omega + \frac{1}{2}\rho, \tag{8}$$

$$\mu_n(n,\alpha) = \sqrt{k_+(n,\alpha)^2 + m_n^*(\sigma,\delta)^{\,2}} + \omega - \frac{1}{2}\rho. \tag{9}$$

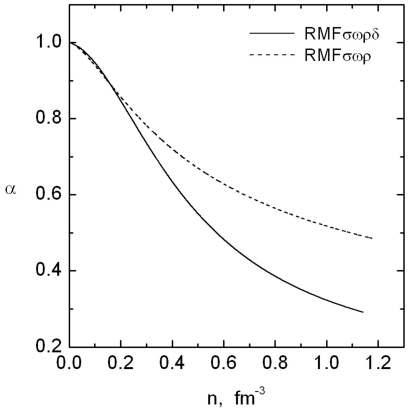

Fig. 1 The asymmetry parameter as a function of the baryon number density n for a β -equilibrium charge-neutral npe -plasma. The solid and dashed curve correspond to the $RMF\sigma\omega\rho\delta$ and $RMF\sigma\omega\rho$ models, respectively.

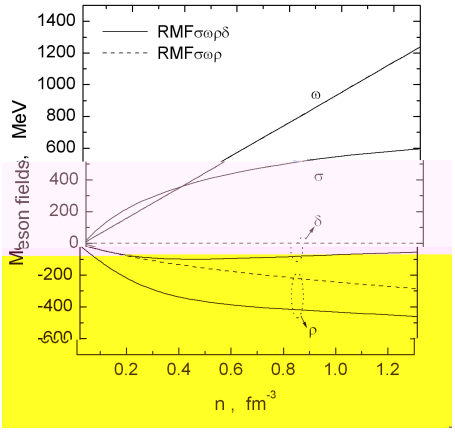

Fig. 2 Re-denoted meson mean-fields as a function of the baryon number density n in case of a β-equilibrium charge-neutral npe-plasma with and without δ-meson field.The solid and dashed curves correspond to the $RMF\sigma\omega\rho\delta$ and $RMF\sigma\omega\rho$ models, respectively.

In Fig.1 we show the asymmetry parameter α for the β -equilibrium charge-neutral npe-plasma, as a function of the baryon number density, n (Alaverdyan 2009a). The solid and dashed curve correspond to the $RMF\sigma\omega\rho\delta$ and $RMF\sigma\omega\rho$ models, respectively. One can see that asymmetry parameter falls off monotonically with the increase of baryon number density n. For a fixed baryon number density n, the inclusion of the δ-meson effective field reduces the asymmetry parameter α. The presence of δ-field reduces the neutron density n_n and increases the proton density n_p.

In Fig.2 we plotted the effective mean-fields of exchanged mesons, σ, ω, ρ and δ as a function of the baryon number density n for the charge-neutral β-equilibrium npe-plasma. The solid and dashed lines correspond to the $RMF\sigma\omega\rho\delta$ and $RMF\sigma\omega\rho$ models, respectively.

From Fig.1 and Fig.2 one can see that the inclusion of the scalar-isovector virtual $\delta(a_0(980))$ meson results in significant changes of species baryon number densities n_p and n_n, as well as the ρ and δ meson effective fields. This can result in changes of deconfinement phase transition parameters and, thus, alter the structural characteristics of neutron stars.

The results of our analysis show that the scalar - isovector δ-meson field inclusion leads to the increase of the EOS stiffness of nuclear matter due to the splitting of proton and neutron effective masses, and also the increase of asymmetry energy (for details see Ref. Alaverdyan 2009a).

2.2 Quark Matter

To describe the quark phase an improved version of the MIT bag model (Chodos et al. 1974) is used, in which the interactions between u, d and s quarks inside the bag are taken into account in the one-gluon

exchange approximation (Farhi & Jaffe 1984). The quark phase consists of three quark flavors u, d, s and electrons, which are in equilibrium with respect to weak interactions. We choose $m_u = 5$ MeV, $m_d = 7$ MeV and $m_s = 150$ MeV for quark masses, and $\alpha_s = 0.5$ for the strong interaction constant.

2.3 Deconfinement Phase Transition Parameters

There are two independent conserved charges in hadron-quark phase transition: baryonic charge and electric charge. The constituents chemical potentials of the npe-plasma in β-equilibrium are expressed through two potentials, $\mu_b^{(NM)}$ and $\mu_{el}^{(NM)}$, according to conserved charges, as follows

$$\mu_n = \mu_b^{(NM)}, \quad \mu_p = \mu_b^{(NM)} - \mu_{el}^{(NM)}, \quad \mu_e = \mu_{el}^{(NM)}. \tag{10}$$

In this case, the pressure P_{NM}, energy density ε_{NM} and baryon number density n_{NM}, are functions of potentials, $\mu_b^{(NM)}$ and $\mu_{el}^{(NM)}$.

The particle species chemical potentials for $udse$-plasma in β-equilibrium are expressed through the chemical potentials $\mu_b^{(QM)}$ and $\mu_{el}^{(QM)}$ as follows

$$\begin{aligned} \mu_u &= \frac{1}{3}\left(\mu_b^{(QM)} - 2\,\mu_{el}^{(QM)}\right), \\ \mu_d &= \mu_s = \frac{1}{3}\left(\mu_b^{(QM)} + \mu_{el}^{(QM)}\right), \\ \mu_e &= \mu_d - \mu_u = \mu_{el}^{(QM)}. \end{aligned} \tag{11}$$

In this case, the thermodynamic characteristics, pressure P_{QM}, energy density ε_{QM} and baryon number density n_{QM}, are functions of chemical potentials $\mu_b^{(QM)}$ and $\mu_{el}^{(QM)}$.

The mechanical and chemical equilibrium conditions (Gibbs conditions) for mixed phase are

$$\mu_b^{(QM)} = \mu_b^{(NM)} = \mu_b, \quad \mu_{el}^{(QM)} = \mu_{el}^{(NM)} = \mu_{el}, \tag{12}$$

$$P_{QM}(\mu_b,\, \mu_{el}) = P_{NM}(\mu_b,\, \mu_{el}). \tag{13}$$

The volume fraction of quark phase is

$$\chi = V_{QM} / \left(V_{QM} + V_{NM}\right), \tag{14}$$

where V_{QM} and V_{NM} are volumes occupied by quark matter and nucleonic matter, respectively.

We applied the global electrical neutrality condition for mixed quark-nucleonic matter, according to Glendenning (Glendenning 1992, 2000),

$$\begin{aligned} (1-\chi)\left[n_p(\mu_b,\mu_{el}) - n_e(\mu_{el})\right] \\ +\chi\left[\frac{2}{3}\,n_u(\mu_b,\mu_{el}) - \frac{1}{3}\,n_d(\mu_b,\mu_{el}) - \frac{1}{3}\,n_s(\mu_b,\mu_{el}) - n_e(\mu_{el})\right] = 0. \end{aligned} \tag{15}$$

The baryon number density in the mixed phase is determined as

$$\begin{aligned} n = (1-\chi)\left[n_p(\mu_b,\mu_{el}) + n_n(\mu_b,\mu_{el})\right] \\ +\frac{1}{3}\,\chi\left[n_u(\mu_b,\mu_{el}) + n_d(\mu_b,\mu_{el}) + n_s(\mu_b,\mu_{el})\right], \end{aligned} \tag{16}$$

and the energy density is

$$\begin{aligned} \varepsilon = (1-\chi)\left[\varepsilon_p(\mu_b,\mu_{el}) + \varepsilon_n(\mu_b,\mu_{el})\right] \\ +\chi\left[\varepsilon_u(\mu_b,\mu_{el}) + \varepsilon_d(\mu_b,\mu_{el}) + \varepsilon_s(\mu_b,\mu_{el})\right] + \varepsilon_e(\mu_{el}). \end{aligned} \tag{17}$$

Table 2 The Mixed Phase Threshold Parameters with and without δ -Meson Field for Bag Parameter Values, $B = 60$ MeV/fm^3 and $B = 100$ MeV/fm^3

Model	n_N (fm^{-3})	n_Q (fm^{-3})	P_N (MeV/fm^3)	P_Q (MeV/fm^3)	ε_N (MeV/fm^3)	ε_Q (MeV/fm^3)
B60$\sigma\omega\rho\delta$	0.0771	1.083	0.434	327.745	72.793	1280.884
B60$\sigma\omega\rho$	0.0717	1.083	0.336	327.747	67.728	1280.889
B100$\sigma\omega\rho\delta$	0.2409	1.448	16.911	474.368	235.029	1889.336
B100$\sigma\omega\rho$	0.2596	1.436	18.025	471.310	253.814	1870.769

In case of $\chi = 0$, the chemical potentials μ_b^N and μ_{el}^N, corresponding to the lower threshold of a mixed phase, are determined by solving Eqs. (13) and (15). This allows to find the lower boundary parameters P_N, ε_N and n_N. Similarly, we calculate the upper boundary values of mixed phase parameters, P_Q, ε_Q and n_Q, for $\chi = 1$. The system of Eqs. (13), (15), (16) and (17) makes it possible to determine EOS of mixed phase between this critical states.

Note, that in the case of an ordinary first-order phase transition both nuclear and quark matter are assumed to be separately electrically neutral, and at some pressure P_0, corresponding to the coexistence of the two phases, their baryon chemical potentials are equal, i.e.,

$$\mu_{NM}(P_0) = \mu_{QM}(P_0). \tag{18}$$

Such phase transition scenario is known as phase transition with constant pressure (Maxwell construction).

Table 2 represents the parameter sets of the mixed phase with and without δ-meson field. It is shown that the presence of δ-field alters the threshold characteristics of the mixed phase. For $B = 60$ MeV/fm^3 the lower threshold parameters, n_N, ε_N and P_N, are increased, meanwhile the upper ones, n_Q, ε_Q and P_Q, are slowly decreased. For $B = 100$ MeV/fm^3 this behavior changes to opposite.

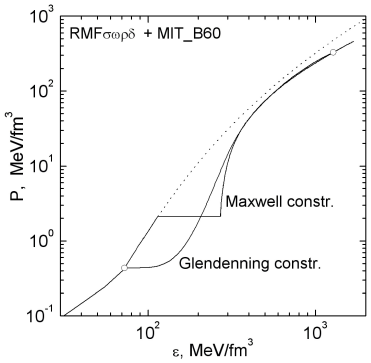

Fig. 3 EOS of neutron star matter with the deconfinement phase transition for a bag constant $B = 60$ MeV/fm^3. For comparison we plot both the Glendenning and Maxwell constructions. Open circles represent the mixed phase boundaries.

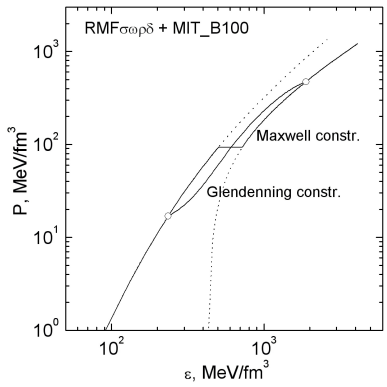

Fig. 4 As in Fig 3, but for $B = 100$ MeV/fm^3.

In Fig.3 and Fig.4 we plot the EOS of compact star matter with deconfinement phase transition for two values of bag constant, $B = 60$ MeV/fm^3 and $B = 100$ MeV/fm^3, respectively. The dotted

curves correspond to pure nucleonic and quark matters without any phase transition, while the solid lines correspond to two alternative phase transition scenarios. Open circles show the boundary points of the mixed phase.

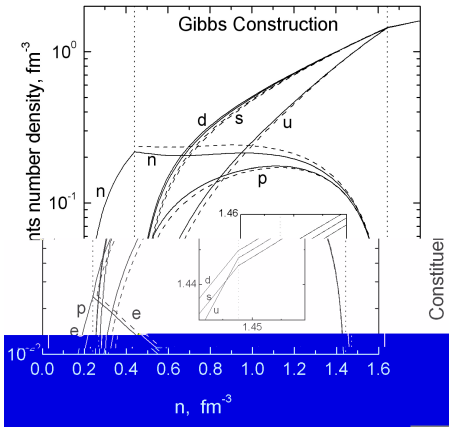

Fig. 5 Constituents number density versus baryon number density n for $B = 100$ MeV/fm^3 in case of Glendenning construction. Vertical dotted lines represent the mixed phase boundaries. The dashed curves show appropriate results of the model without δ-meson field.

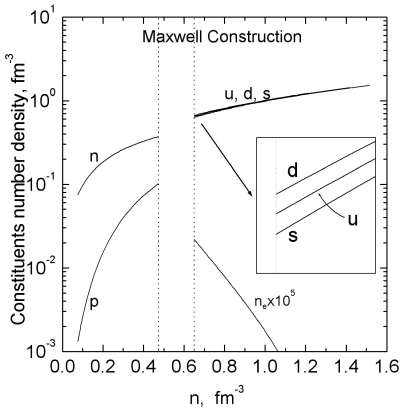

Fig. 6 As in Fig 5, but for Maxwell construction. Vertical dotted lines represent the density jump boundaries.

In Fig.5 we plot the particle species number densities as a function of baryon density n for Glendenning construction. Quarks appear at the critical density $n_N = 0.241$ fm^{-3}. The hadronic matter completely disappears at $n_Q = 1.448$ fm^{-3}, where the pure quark phase occurs. The solid curves correspond to the case, when also the δ- meson effective field is taken into account besides σ, ω, ρ meson fields (model $B100\_\sigma\omega\rho\delta$). The dashed curves represent the results in case when we neglect the δ-meson field (model $B100\_\sigma\omega\rho$). One can see that inclusion of the δ-meson field leads to the increase of number densities of quarks and protons, and simultaneously to the reduction of number densities of neutrons and electrons. In Table 2 we have already shown the mixed phase boundaries changes caused by the inclusion of the δ - meson effective field.

Fig.6 shows the constituents number density as a function of baryon number density n for $B = 100$ MeV/fm^3, when phase transition is described according to Maxwell construction. Maxwell construction leads to the appearance of a discontinuity. In this case, the charge neutral nucleonic matter at baryon density $n_1 = 0.475$ fm^{-3} coexists with the charge neutral quark matter at baryon density $n_2 = 0.650$ fm^{-3}. Thus, the density range $n_1 < n < n_2$ is forbidden. In case of Maxwell construction, the chemical potential of electrons, μ_e, has a jump at the coexistence pressure P_0. Notice, that such discontinuity behavior takes place only in usual first-order phase transition, i.e., in the Maxwell construction case.

3 PROPERTIES OF HYBRID STARS

Using the EOS obtained in previous section, we calculate the integral and structural characteristics of neutron stars with quark degrees of freedom.

The hydrostatic equilibrium properties of spherical symmetric and isotropic compact stars in general relativity is described by the Tolman-Oppenheimer-Volkoff(TOV) equations (Tolman 1939; Oppenheimer & Volkoff 1939):

$$\frac{dP}{dr} = -\frac{G}{r^2}\frac{(P+\varepsilon)(m+4\pi r^3 P)}{1-2G\,m/r}, \tag{19}$$

$$\frac{dm}{dr} = 4\pi r^2 \varepsilon, \tag{20}$$

where G is the gravitational constant, r is the distance from the center of star, $m(r)$ is the mass inside a sphere of radius r, $P(r)$ and $\varepsilon(r)$ are the pressure and energy density at the radius r, respectively. To integrate the TOV equations, it is necessary to know the EOS of neutron star matter in a form $\varepsilon(P)$. Using the neutron star matter EOS, obtained in previous section, we have integrated the Tolman-Oppenheimer Volkoff equations and obtained the gravitational mass M and the radius R of compact stars (with and without quark degrees of freedom) for the different values of central pressure, P_c.

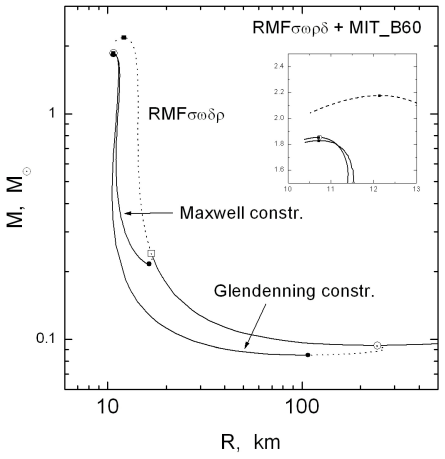

Fig. 7 The mass-radius relation of neutron star with different deconfinement phase transition scenarios for the bag constant $B = 60$ MeV/fm^3. Open circles and squares denote the critical configurations for Glendenning and Maxwellian type transitions, respectively. Solid circles and squares denote hybrid stars with minimal and maximal masses, respectively.

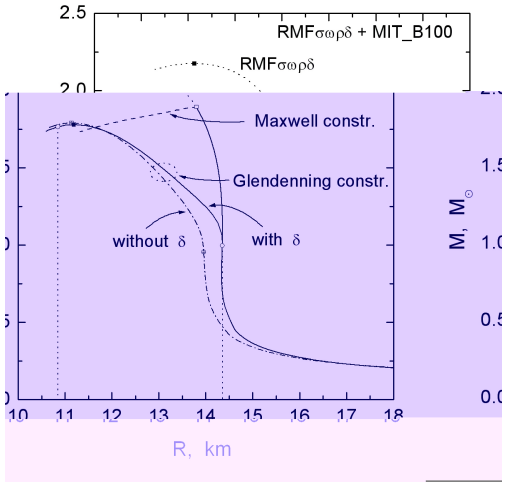

Fig. 8 As in Fig 7, but for $B = 100$ MeV/fm^3. The mass-radius relation in case of the Glendennig construction without the δ-meson effective field is also displayed for comparison (dash-dotted curve).

Fig.7 and Fig.8 illustrate the $M(R)$ dependence of neutron stars for the two values of bag constant $B = 60$ MeV/fm^3 and $B = 100$ MeV/fm^3, respectively. We can see, that the behavior of mass-radius dependence significantly differs for the two types of phase transitions. Fig.7 shows, that for $B = 60$ MeV/fm^3 there are unstable regions, where $dM/dP_c < 0$ between two stable branches of compact stars, corresponding to configurations with and without quark matter. In this case, there is a nonzero minimum value of the quark phase core radius. Accretion of matter on a critical neutron star configuration will then result in a catastrophic rearrangement of the star, forming a star with a quark matter core. The range of mass values for stars, containing the mixed phase, is $[0.085M_\odot; 1.853M_\odot]$ for $B = 60$ MeV/fm^3, and is $[0.997M_\odot; 1.780M_\odot]$ for $B = 100$ MeV/fm^3. In case of Maxwellian type phase transition, the analogous range is $[0.216M_\odot; 1.828M_\odot]$ for $B = 60$ MeV/fm^3. From Fig.8 one can observe, that in case of $B = 100$MeV/fm^3, the star configurations with deconfined quark matter are unstable. Thus, the stable neutron star maximum mass is $1.894M_\odot$. Our analysis show, that for $B = 100$MeV/fm^3, the pressure upper threshold value for mixed phase is larger than the pressure, corresponding to the maximum mass configuration. Hence, in this case, the mixed phase can exist in the center of compact stars, but no pure quark matter can exist. The dash-dotted curve in Fig.8 represents the results in case when we neglect the δ-meson field (model $B100\_\,\sigma\omega\rho$). One can see that for a fixed gravitational

Table 3 Hybrid Star Critical Configuration Properties for $B = 100$ MeV/fm^3 with and without δ-Meson Field

	Minimum Mass Configuration			Maximum Mass Configuration		
Model	ε_c (MeV/fm^3)	M_{min} ($M_\odot$)	R (km)	ε_c (MeV/fm^3)	M_{max} ($M_\odot$)	R (km)
B100$\sigma\omega\rho\delta$	235.029	0.997	14.354	1390.77	1.780	11.190
B100$\sigma\omega\rho$	253.814	0.955	13.960	1386.03	1.791	11.139

mass the star with δ-meson field has larger radius than the corresponding star without the δ-meson field. Influence of δ-meson field on the hybrid star properties is demonstrated in Table 3, where we display the hybrid star properties with and without δ-meson field for minimum and maximum mass configurations. The results show that the minimum mass of hybrid stars and corresponding radius are increased with the inclusion of the δ-meson field. Notice that influence of δ-meson field on maximum mass configuration properties is insignificant.

4 CONCLUSIONS

In this paper we have studied the deconfinement phase transition of neutron star matter, when the nuclear matter is described in the RMF theory with δ-meson effective field. We show that the inclusion of scalar isovector δ-meson field terms leads to the stiff nuclear matter EOS. In a nucleonic star both the gravitational mass and corresponding radius of the maximum mass stable configuration increases with the inclusion of the δ field. The presence of scalar isovector δ-meson field alters the threshold characteristics of the mixed phase. For $B = 60$ MeV/fm^3, the lower threshold parameters, n_N, ε_N, P_N, are increased, meanwhile the upper ones, n_Q, ε_Q, P_Q, are slowly decreased. For $B = 100$ MeV/fm^3 this behavior changes to opposite.

In case of the bag constant value $B = 100$MeV/fm^3, the pressure upper threshold value for mixed phase is larger, than the pressure, corresponding to the maximum mass configuration. This means that in this case, the stable compact star can possess a mixed phase core, but the density range does not allow to possess a pure strange quark matter core.

Stars with δ-meson field have larger radius than stars of the same gravitational mass without the δ-meson field. Alterations of the maximum mass configuration parameters caused by the inclusion of δ-meson field is insignificant.

For the bag constant value $B = 60$ MeV/fm^3, the maximum mass configuration has a gravitational mass $M_{max} = 1.853\ M_\odot$ with radius $R = 10.71$ km, and central density $\rho_c = 2.322 \cdot 10^{15}$ g/cm^3. This star has a pure strange quark matter core with radius $r_Q \approx 0.83$ km, next it has a nucleon-quark mixed phase layer with a thickness of $r_{MP} \approx 9.43$ km, followed by a normal nuclear matter layer with a thickness of $r_N \approx 0.45$ km.

Acknowledgements The author would like to thank Profs. Yu.L.Vartanyan and G.S.Hajyan for fruitful discussions on issues related to the subject of this research.

This work was partially supported by the Ministry of Education and Sciences of the Republic of Armenia under grant 2008-130.

References

Alaverdyan, G. B. 2009a, Astrophysics, 52, 132
Alaverdyan, G. B. 2009b, Gravitation & Cosmology, 15, 5
Baym, G., Bethe, H. Pethick, Ch. 1971, Nucl.Phys. A175, 255
Boguta J. & Bodmer, A. R. 1977, Nucl.Phys. A 292, 413
Chodos, A., Jaffe, R. L., Johnson, K., Thorn, C. B., Weisskopf, V. F. 1974, Phys.Rev. D 9, 3471.
Farhi, E., Jaffe, R. L., 1984, Phys.Rev. D 30, 2379

Glendenning, N. K. 1992, Phys. Rev. D 46, 1274
Glendenning, N. K. 2000, Compact Stars, (New York: Springer)
Greco, V., Colonna, M., Di Toro, M., Matera, F. 2003, Phys. Rev. C 67, 015203
Heiselberg, H., Pethick, C. J., Staubo, E. S. 1993, Phys. Rev. Lett. 70, 1355
Heiselberg, H. & Hjorth-Jensen, M. 1999, arXiv: 9902033 v1, [nucl-th]
Ko, C. M., Li, G. Q. 1996, Journal of Phys. G 22, 1673
Kubis, S., Kutschera, M., 1997, Phys. Lett., B 399, 191
Lalazissis, G. A., Konig, J. & Ring, P. 1997, Phys.Rev. C 55, 540
Liu, B., Greco, V., Baran, V., Colonna, M., Di Toro, M. 2002, Phys.Rev. C 65, 045201
Miller, H., Serot, B. D., Phys. Rev. C 52, 2072
Oppenheimer, J. & Volkoff, G. 1939, Phys.Rev. 55, 374
Prassa, V., Ferini, G., Gaitanos, T., Wolter, H. H., Lalazissis, G. A. & Di Toro, M. 2007, ArXiv e-prints (arXiv:0704.0554)
Serot, B. D. & Walecka, J. D. 1986, in: Adv. in Nucl. Phys., eds. J. W. Negele & E. Vogt, vol. 16
Serot, B. D., Walecka, J. D. 1997, Int.J.Mod.Phys. E6, 515
Tolman, R. 1939, Phys.Rev. 55, 364
Typel, S., Wolter, H. H. 1999, Nucl. Phys. A 656, 331
Walecka, J. D. 1974, Ann. Phys., 83, 491